RSC Advances

PAPER

View Article Online
View Journal | View Issue

Cite this: *RSC Adv.*, 2017, **7**, 27415

Phase evolution and microwave dielectric properties of ceramics with nominal composition $Li_{2x}(Zn_{0.95}Co_{0.05})_{2-x}SiO_4$ for LTCC applications

Xiangyu Du,[a] Hua Su,[ab] *[ab] Huaiwu Zhang,[a] Xiuting Liu[a] and Xiaoli Tang[a]

Received 27th March 2017
Accepted 17th May 2017

DOI: 10.1039/c7ra03523c

rsc.li/rsc-advances

$Li_{2x}(Zn_{0.95}Co_{0.05})_{2-x}SiO_4$ ($0 \le x \le 1$) ceramics were prepared through the conventional solid-state route. A fixed amount of Li_2O–MgO–ZnO–B_2O_3–SiO_2 (LMZBS) glass was used as a sintering aid to help lower the sintering temperature to around 900 °C. The effects of part lithium-ion substitution on the phase formation, sintering behaviour, microstructures and microwave dielectric properties of the ceramics were systematically investigated. When $x = 0.25$, the sample achieved a dense microstructure and exhibited excellent microwave dielectric properties of $\varepsilon_r = 6.47$, $Q \times f = 131\,579$ GHz and $\tau_f = -27.12$ ppm °C^{-1}. For its practical application in low-temperature co-fired ceramics (LTCC), large positive τ_f of $CaTiO_3$ was used to adjust the τ_f value of the composite ceramic to nearly zero. The composite ceramic of $0.975Li_{0.5}(Zn_{0.95}Co_{0.05})_{1.75}SiO_4$–$0.025CaTiO_3$ sintered at 900 °C also presented good microwave dielectric properties of $\varepsilon_r = 6.773$, $Q \times f = 69\,177$ GHz and $\tau_f = -2.45$ ppm °C^{-1}.

1. Introduction

Microwave dielectric materials are widely investigated for their extensive applications as filters, duplexers and antennas in microwave communication industries.[1,2] Materials with low permittivity (ε_r), high quality factor ($Q \times f$) and near-zero temperature coefficient of resonant frequency (τ_f) are required to reduce cross-talk, propagation delay time, noise and power dissipation.[3–5] Furthermore, these materials should be sintered at temperatures lower than 950 °C or even 900 °C to be used in LTCC multi-layer devices for the miniaturisation and integration of microwave components because of silver (Ag) electrode (around 961 °C), which is typically used as metallic electrode in LTCC materials.[6,7] Although a number of materials (such as Al_2O_3 (ref. 4), $MgTiO_3$ (ref. 8) and Mg_2SiO_4 (ref. 3)) have low permittivity and dielectric loss, these materials cannot be used in LTCC multi-layer devices because of the high sintering temperature.[9] Zn_2SiO_4 is one of these materials and has a low dielectric constant (6.6), a high quality factor value (219 000 GHz) and a temperature coefficient of resonant frequency of −61 ppm °C^{-1}. Analogously, the high sintering temperature of 1340 °C limits the application of Zn_2SiO_4 in LTCC technology.[10]

Recently, Chen reported that the co-substitution $(Zn_{1-x}Co_x)_2SiO_4$ ceramics lowers the sintering temperature of Zn_2SiO_4 from 1340 °C to 1300 °C and restrains the formation of ZnO phase.[11] Zhou lowered the sintering temperature of $(Zn_{0.95}Co_{0.05})_2SiO_4$ ceramics to 900 °C by adding 1.5 wt% LBBS glass. The ceramics sintered at 900 °C showed $\varepsilon_r = 6.16$, $Q \times f = 33\,000$ GHz and $\tau_f = -59$ ppm °C^{-1}.[12] Nonetheless, the ceramics have a large negative τ_f value, which restricts its potential for practical application. Furthermore, the quality factor is still too low to keep up with the high-speed development of LTCC technology. Although the addition of low softening point glass is the most inexpensive way to lower the sintering temperature of dielectric ceramics, previous studies concluded that a large amount of glass addition leads to either high microwave dielectric loss or crack formation.[13] Hence, new strategies combined with low amount of sintering aids should be developed to further lower the sintering temperature and dielectric loss of $(Zn_{0.95}Co_{0.05})_2SiO_4$ ceramics.

The lithium-substitution on Li_2CaSiO_4,[14] $LiAlSiO_4$ (ref. 15) and Li_2MgSiO_4 (ref. 16) ceramics presented good dielectric properties of low dielectric constant (<10) and high $Q \times f$ value. However, the phase evolution, sintering behaviour and optimal lithium-substitution content on $(Zn_{0.95}Co_{0.05})_2SiO_4$ ceramics are not yet reported. Therefore, in this work, the ceramics with nominal composition $Li_{2x}(Zn_{0.95}Co_{0.05})_{2-x}SiO_4$ was synthesised to systematically study the phase formation, sintering behaviour, microstructures and microwave dielectric properties. A fixed amount of LMZBS glass was used as a sintering aid to help lower the sintering temperature at around 900 °C. Moreover, a common modifier with large positive τ_f of $CaTiO_3$ was used to adjust the τ_f value of the ceramic, which exhibited the best microwave dielectric property, in the ceramics with nominal composition $Li_{2x}(Zn_{0.95}Co_{0.05})_{2-x}SiO_4$ to nearly zero, thereby

[a]State Key Laboratory of Electronic Thin Films and Integrated Devices, University of Electronic Science and Technology of China, Chengdu 610054, China. E-mail: uestcsh77@163.com

[b]Institute of Electronic and Information Engineering, University of Electronic Science and Technology of China, Dongguan 518105, China

making these ceramics promising candidates for LTCC materials.

2. Experimental

2.1. Preparation of ceramic samples

$Li_{2x}(Zn_{0.95}Co_{0.05})_{2-x}SiO_4$ ($0 \le x \le 1$) ceramics were prepared through the traditional solid-state ceramic route. The schematic plot of the fabrication process of ceramics is shown in Fig. 1. A previous study reported that the cobalt ions substituted for zinc ions in the lattice sites of ZnO exist as Co^{2+} ions when Co_2O_3 was used as raw powders.[17] Hence, high-purity oxides Li_2CO_3 (99%), ZnO (99%), SiO_2 (99%), Co_2O_3 (99%), $CaCO_3$ (99%) and TiO_2 (99%) were used as the raw materials. These raw powders, which were weighed according to respective stoichiometric ratio of $Li_{2x}(Zn_{0.95}Co_{0.05})_{2-x}SiO_4$ ($0 \le x \le 1$) and $CaTiO_3$, were ball-milled in nylon jars with zirconia balls in distilled water for 6 h. The resultant slurry was dried, sieved and calcined at 1050 °C for 4 h and 1100 °C for 3 h in air, respectively. A fixed amount of 1.5 wt% LMZBS glass was doped to the pre-sintered $Li_{2x}(Zn_{0.95}Co_{0.05})_{2-x}SiO_4$ ($0 \le x \le 1$) powders and then re-milled in distilled water medium for 12 h. With 25 wt% polyvinyl alcohol (PVA) solution as a binder, the powders were dried at 120 °C, well-ground, granulated and pressed into disks under a pressure of 9 MPa and then sintered at 850 °C to 950 °C for 3 h.

After determining the optimal x value to obtain the best microwave dielectric properties of $Li_{2x}(Zn_{0.95}Co_{0.05})_{2-x}SiO_4$ ($0 \le x \le 1$) ceramics sintered at 900 °C, different amounts of pre-sintered $CaTiO_3$ powders were added to $Li_{2x}(Zn_{0.95}Co_{0.05})_{2-x}SiO_4$ (x was determined) powders with 1.5 wt% LMZBS glass to adjust the τ_f value of $Li_{2x}(Zn_{0.95}Co_{0.05})_{2-x}SiO_4$ ceramic to nearly zero. The subsequent process was similar to the above-mentioned procedure.

2.2. Preparation of glass

The Li_2O–MgO–ZnO–B_2O_3–SiO_2 (LMZBS) glass was synthesised using a quenching method. High-purity grade raw materials (>99%) were mixed, ball-milled and melted at 1350 °C for 1 h using an alumina crucible at the molar ratio of Li_2CO_3 : MgO:ZnO : B_2O_3 : SiO_2 = 20 : 20 : 20 : 20 : 20. The solution was quickly removed from the furnace and was quenched with cold distilled water to obtain the glass.

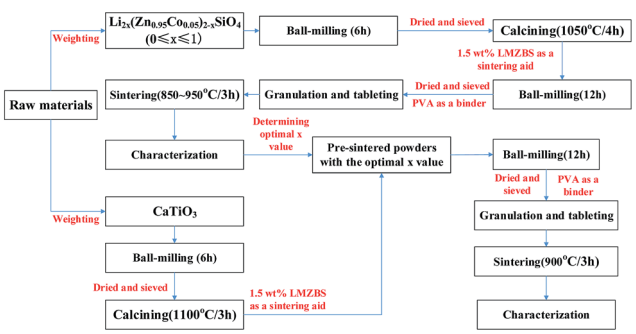

Fig. 1 Schematic plot of the fabrication process of ceramics.

2.3. Sample characterization

The bulk densities of these sintered specimens were measured using the Archimedes method. Relative densities were obtained by using the ratio of the bulk and theoretical densities. The phase compositions of theses sintered samples were determined by X-ray diffraction (XRD:DX-2700) using Cu Kα radiation. The microstructure of the ceramics was examined by scanning electron microscopy (SEM: Hitachi S-3400N). The microwave dielectric properties of the sintered specimens were investigated using an Agilent N5230A network analyser (300 MHz to 20 GHz) in a resonant cavity. The quality factor and relative permittivity were measured by the resonant-cavity method and the Hakki–Coleman method, respectively.[18] The temperature coefficient of resonant frequency (τ_f) was measured from the invar cavity using the following formula in the temperature range of 20–80 °C:[19]

$$\tau_f = \frac{f_T - f_0}{f_0(T - T_0)} \times 10^6 \quad (1)$$

where f_T and f_0 are the resonant frequencies at 80 °C and 20 °C, T and T_0 are 80 °C and 20 °C, respectively.

3. Results and discussion

Fig. 2a shows the XRD diffraction patterns of $Li_{2x}(Zn_{0.95}Co_{0.05})_{2-x}SiO_4$ ($0 \le x \le 1$) ceramics doped with 1.5 wt% LMZBS and sintered at 900 °C for 3 h in air. Fig. 2b shows the schematic plot of phase evolution of $Li_{2x}(Zn_{0.95}Co_{0.05})_{2-x}SiO_4$ with various amounts of lithium-ion substitution. Only a rhombohedral structure $(Zn,Co)_2SiO_4$ phase (●, PDF #46-1316) appeared in the XRD pattern of the sample with no lithium doped. However, when $0.125 \le x \le 0.625$, the $Li_{1.6}Zn_{1.2}SiO_4$ phase (◆, PDF #24-0676) co-existed with $(Zn,Co)_2SiO_4$ phase in the sintered samples. The peak intensities of $Li_{1.6}Zn_{1.2}SiO_4$ phase gradually increased with the increasing x value. When $0.125 \le x \le 0.375$, the crystalline phase of $(Zn,Co)_2SiO_4$ was the main phase, and the phase of $Li_{1.6}Zn_{1.2}SiO_4$ was the minor phase. However, both of the crystalline phases became the main phase when x was increased to 0.5. When the x value exceeded 0.625, the phase of $(Zn,Co)_2SiO_4$ disappeared (Fig. 2a(g)), and another two crystalline phases of tetragonal structure Li_2ZnSiO_4 (*, PDF #15-0056) and orthorhombic structure Li_2CoSiO_4 (▽, PDF #24-0611) appeared in the sintered sample when $x = 1$ (Fig. 2a(h)). Fig. 2 shows that various amounts of lithium-ion substitution induce different phase-formations in $Li_{2x}(Zn_{0.95}Co_{0.05})_{2-x}SiO_4$ ($0 \le x \le 1$) ceramics.

Fig. 3 illustrates the SEM images of samples doped with 1.5 wt% LMZBS glass and sintered at 900 °C with various x values. Generally, the microstructures present considerable densification that might be due to the sufficient liquid phase, which resulted from the glass addition. In detail, with the increasing x value to 0.25, the pores decreased, and the grain was enlarged (see Fig. 2a–c). Combined with the XRD patterns shown in Fig. 2a, this finding explained that a moderate amount of Li substitution might reduce the sintering temperature of the ceramics with nominal composition $Li_{2x}(Zn_{0.95}Co_{0.05})_{2-x}SiO_4$

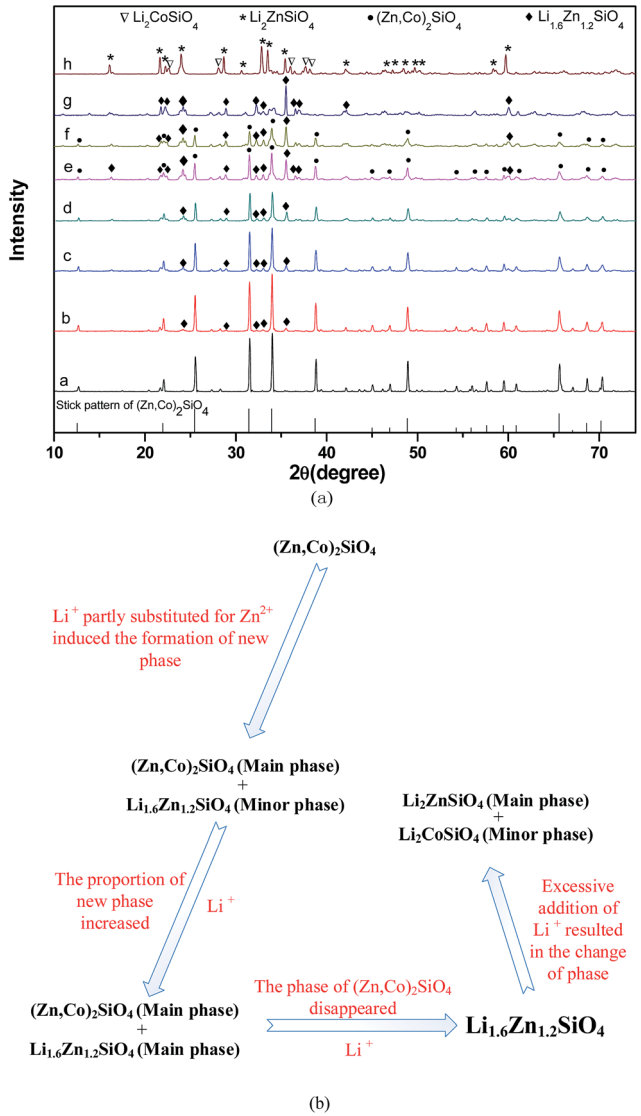

Fig. 2 (a) XRD diffraction patterns of $Li_{2x}(Zn_{0.95}Co_{0.05})_{2-x}SiO_4$ ($0 \le x \le 1$) ceramics doped with 1.5 wt% LMZBS and sintered at 900 °C for 3 h. (a) $x = 0$, (b) $x = 0.125$, (c) $x = 0.25$, (d) $x = 0.375$, (e) $x = 0.5$, (f) $x = 0.625$, (g) $x = 0.75$, and (h) $x = 1$. (b) Schematic plot of phase evolution of $Li_{2x}(Zn_{0.95}Co_{0.05})_{2-x}SiO_4$ with various amounts of lithium-ion substitution.

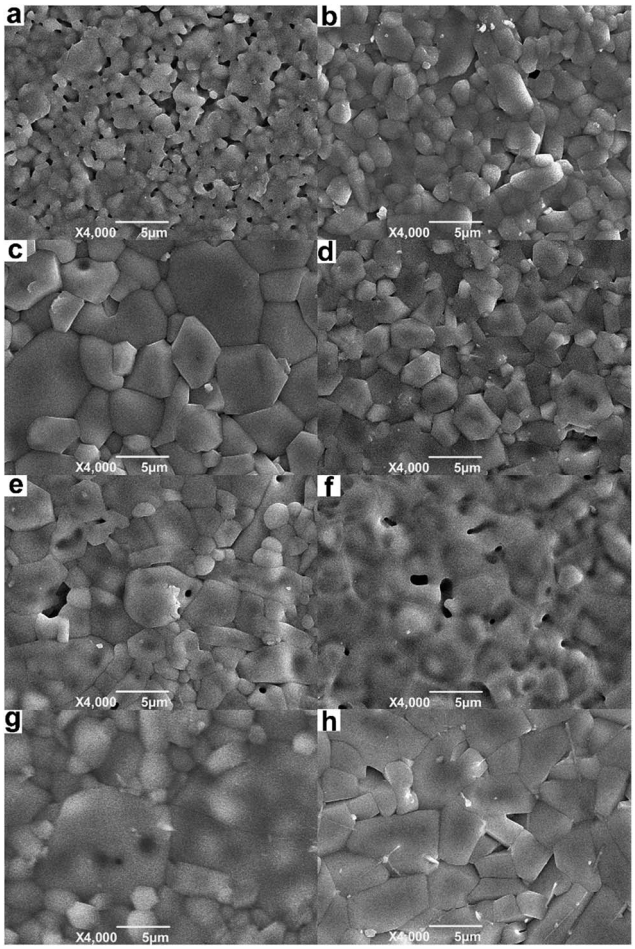

Fig. 3 SEM micrographs of $Li_{2x}(Zn_{0.95}Co_{0.05})_{2-x}SiO_4$ ($0 \le x \le 1$) ceramics doped with 1.5 wt% LMZBS and sintered at 900 °C for 3 h. (a) $x = 0$, (b) $x = 0.125$, (c) $x = 0.25$, (d) $x = 0.375$, (e) $x = 0.5$, (f) $x = 0.625$, (g) $x = 0.75$, and (h) $x = 1$.

via synthesising $Li_{1.6}Zn_{1.2}SiO_4$. The sintering temperature of $(Zn_{0.95}Co_{0.05})_2SiO_4$ was 1300 °C, which is almost similar to that of Zn_2SiO_4.[10,12] It was reported that lithium-ions partly substituted for metal cations significantly reduced the sintering temperature compared with that of initial silicate materials.[15,16,20] Hence, the sintering temperature of $Li_{1.6}Zn_{1.2}SiO_4$ was lower than that of $(Zn_{0.95}Co_{0.05})_2SiO_4$. However, with the successive addition of lithium, the pores increased (Fig. 3d–f), and a large amount of liquid phase (see Fig. 3f) and evident closed pores in the grains (see Fig. 3e) were observed. These phenomena are attributed to the fast growth of the grains; thus, some pores were trapped in the bodies of the abnormal growth grains.[21] In addition, the liquid phase implied that lithium-ion substitution reduces the sintering temperature and thereby resulted in excessive liquid phase. When $x = 0.75$, a dense microstructure reappeared; however, the abnormal growth grain with closed pores and the liquid phase were still observed in Fig. 3g. When x was increased to 1, the shape of grains became rectangular, and the intergranular pores increased (Fig. 3h). This outcome is attributed to the formation of tetragonal structure of Li_2ZnSiO_4. The optimal content of Li^+ substitution was set at 0.25 to obtain the most compact and uniform microstructure.

Fig. 4 shows the relative density as a function of x value for $Li_{2x}(Zn_{0.95}Co_{0.05})_{2-x}SiO_4$ ($0 \le x \le 1$) specimens doped with 1.5 wt% LMZBS glass and sintered at 850–950 °C for 3 h. The relative density was calculated using the formula $\rho_r = \frac{\rho}{\rho_x}$, where ρ and ρ_x are the bulk and theoretical density values, respectively. The theoretical density ρ_x was calculated as follows:

$$\rho_x = (w_1 + w_2 + w_3) \Big/ \left(\frac{w_1}{\rho_{x1}} + \frac{w_2}{\rho_{x2}} + \frac{w_3}{\rho_{x3}}\right) \quad (2)$$

where w_1, w_2 and w_3 are the weight percentages of crystalline phases and LMZBS glass in $Li_{2x}(Zn_{0.95}Co_{0.05})_{2-x}SiO_4$ ($0 \le x \le 1$)

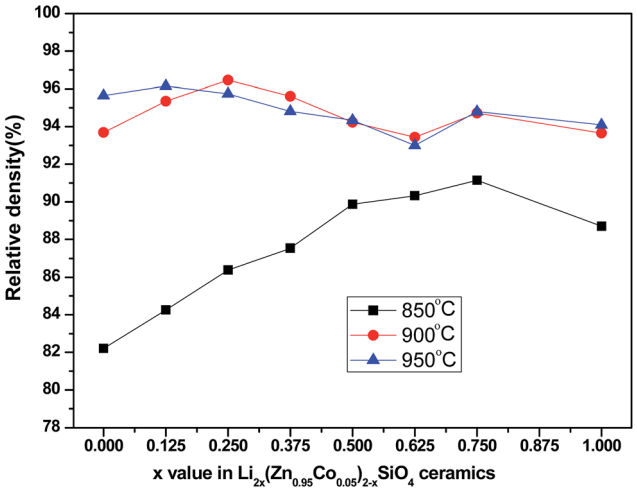

Fig. 4 Relative density of $Li_{2x}(Zn_{0.95}Co_{0.05})_{2-x}SiO_4$ ($0 \leq x \leq 1$) ceramics doped with 1.5 wt% LMZBS glass and sintered at 850–950 °C for 3 h.

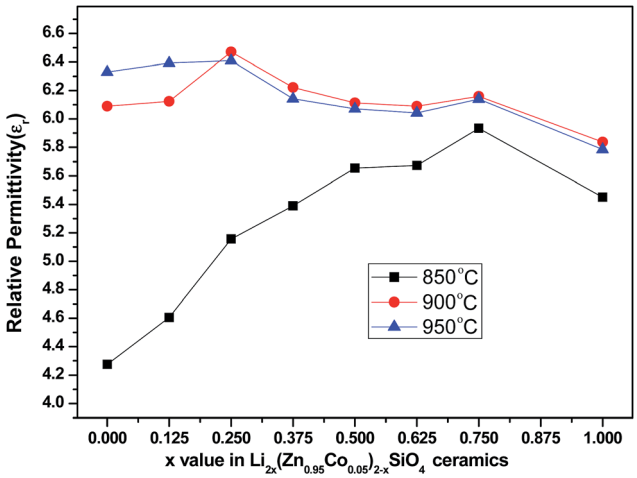

Fig. 5 Relative permittivity (ε_r) of $Li_{2x}(Zn_{0.95}Co_{0.05})_{2-x}SiO_4$ ($0 \leq x \leq 1$) ceramics doped with 1.5 wt% LMZBS glass and sintered at 850–950 °C for 3 h.

ceramics, respectively. The weight percentages of crystalline phases and LMZBS glass were obtained from the XRD analysis and were set at 1.5 wt%. Here, 2.75 g cm^{-3} was used as the theoretical density of LMZBS glass.[22]

The relative density values of samples sintered at 900 °C generally exceed 93%, which implies that 1.5 wt% LMZBS is sufficient to obtain the liquid-phase sintering necessary for the relative densification at 900 °C. When a small amount of lithium was doped to the sample sintered at 900 °C, the relative density increased to 96.46%, which is a fairly high densification. This outcome indicates that a moderate amount of lithium-substitution help facilitate densification. The tendency of relative density of these samples sintered at 900 °C is also consistent with the variations in the microstructure. The relative densities of specimens sintered at 850 °C were significantly lower than those sintered at 900 °C and 950 °C. This phenomenon is attributed to two reasons. One reason is the tight relationship between the sintering temperature and relative density.[23] The other reason is that the softening temperature of LMZBS is around 900 °C, which is higher than the sintering temperature of these samples.[22] Furthermore, a lower sintering temperature shifts the obtainable maximum relative density to higher lithium doped content. This outcome suggested that the substitution of lithium ions markedly lowers the sintering temperature of the ceramics with nominal composition $Li_{2x}(Zn_{0.95}Co_{0.05})_{2-x}SiO_4$.

Fig. 5 shows the relative permittivity (ε_r) values of the $Li_{2x}(Zn_{0.95}Co_{0.05})_{2-x}SiO_4$ ($0 \leq x \leq 1$) ceramics doped with 1.5 wt% LMZBS glass and sintered at 850–950 °C for 3 h. The variation in relative permittivity of specimens sintered at 850–950 °C is generally in agreement with the trend of the relative density. Densification plays a crucial role in determining the relative permittivity.[24] The ε_r of $Li_{2x}(Zn_{0.95}Co_{0.05})_{2-x}SiO_4$ ($0 \leq x \leq 1$) ceramics sintered at 900 °C increased with the increasing x value, reached a maximum value (6.47) at $x = 0.25$ and then decreased to a minimum value (5.84) at $x = 1$. The relative density of the sample sintered at 900 °C (93.69%) when $x = 0$ is similar to that of the sample sintered at the same temperature (93.66%) when $x = 1$, whereas the ε_r when $x = 0$ was obviously higher than when $x = 1$ (6.09 and 5.83, respectively). Combined with the XRD patterns shown in Fig. 2a, this finding is due to the synthesis of Li_2ZnSiO_4, which exists as the major phase. The ε_r of Li_2ZnSiO_4 is 5.8, which is lower than that of $(Zn_{0.95}Co_{0.05})_2SiO_4$ (6.16).[12,20]

Fig. 6 shows the variations in $Q \times f$ values of $Li_{2x}(Zn_{0.95}Co_{0.05})_{2-x}SiO_4$ ($0 \leq x \leq 1$) ceramics with different x contents doped with 1.5 wt% LMZBS and sintered at 850–950 °C for 3 h. The variations in $Q \times f$ values are generally consistent with the variations in the relative density of $Li_{2x}(Zn_{0.95}Co_{0.05})_{2-x}SiO_4$ ($0 \leq x \leq 1$) ceramics. The $Q \times f$ values were all low when the samples were sintered at 850 °C (less than 49 000 GHz), which is mainly attributed to the low relative densities. When the sintering temperature was increased to 900 °C, the $Q \times f$ values

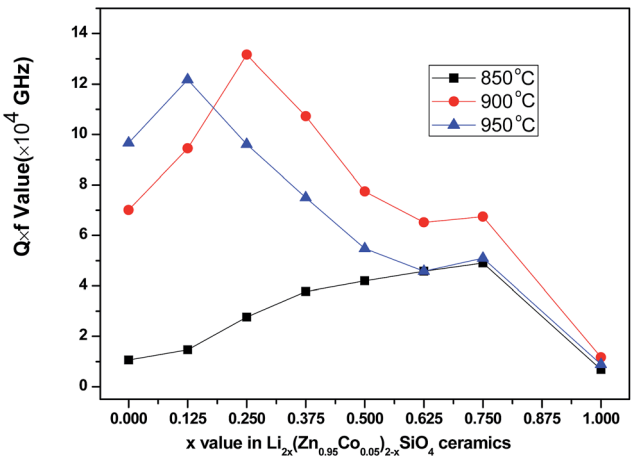

Fig. 6 $Q \times f$ values of $Li_{2x}(Zn_{0.95}Co_{0.05})_{2-x}SiO_4$ ($0 \leq x \leq 1$) ceramics with the addition of 1.5 wt% LMZBS glass sintered at 850–950 °C for 3 h.

increased with the increasing x value and achieved the maximum of 131 579 GHz at $x = 0.25$. This outcome might be due to the high densification (96.46%) of the sintered sample when $x = 0.25$. According to the SEM images shown in Fig. 3c, the large grain resulted in less grain boundary, which indicates less lattice mismatch and lower dielectric loss.[25] The $Q \times f$ values of the samples sintered at 850–950 °C remarkably decreased to the minimal values of around 6800 GHz with the variation in x from 0.75 to 1. Microwave dielectric loss can be divided into intrinsic and extrinsic losses.[26] Intrinsic losses are mainly dependent on the crystal structure and are usually caused by the lattice vibration modes.[27] According to the XRD analysis shown in Fig. 2a, tetragonal structure Li_2ZnSiO_4 (*, PDF #15-0056) was the major phase of the sintered sample when $x = 1$. In a previous study, Li_2ZnSiO_4 ceramics doped with 25 wt% ZB glass sintered at 950 °C exhibited a $Q \times f$ value of 10 800 GHz, which is approximated to the $Q \times f$ value in the present work.[20] Hence, in addition to the influence of extrinsic losses caused by lower densification, the high intrinsic losses of Li_2ZnSiO_4 thereby induced the dramatic decrease of $Q \times f$ values.

Fig. 7 shows the τ_f values of the $Li_{2x}(Zn_{0.95}Co_{0.05})_{2-x}SiO_4$ ($0 \leq x \leq 1$) ceramics with different x values doped with 1.5 wt% LMZBS and sintered at 900 °C for 3 h. The τ_f values initially increased and then decreased with the increasing x content. The temperature coefficient of composite ceramics was obtained from the following logarithmic rule:[28]

$$\tau_f = v_1\tau_{f1} + v_2\tau_{f2} \quad (3)$$

where τ_{f1} and τ_{f2} are the τ_f values of the $(Zn_{0.95}Co_{0.05})_2SiO_4$ and $Li_{1.6}Zn_{1.2}SiO_4$, respectively. The τ_f value of the sample, whose main crystalline phase was the phase of $Li_{1.6}Zn_{1.2}SiO_4$ (when $x = 0.75$), was -9.04 ppm °C^{-1}; while the τ_f value of $(Zn_{0.95}Co_{0.05})_2SiO_4$ was -51.54 ppm °C^{-1}. Hence, the τ_f value of $Li_{1.6}Zn_{1.2}SiO_4$ was higher than that of $(Zn_{0.95}Co_{0.05})_2SiO_4$. Combined with the XRD patterns shown in Fig. 2a and function (3), the volume percentage of $Li_{1.6}Zn_{1.2}SiO_4$ gradually increased by increasing x to 0.75, which might be the reason for the increase of the τ_f values of composite ceramics when $0 \leq x \leq 0.75$. Analogously, when the τ_f values of Li_2ZnSiO_4 was -96.6 ppm °C^{-1}, the τ_f values of $Li_{2x}(Zn_{0.95}Co_{0.05})_{2-x}SiO_4$ ($0.75 \leq x \leq 1$) ceramics decreased with the excessive x content.[20]

Considering the above-mentioned analysis, the optimal x value was set at 0.25 because of the best quality factor of $Li_{0.5}(Zn_{0.95}Co_{0.05})_{1.75}SiO_4$. One of the most important dielectric properties when considering the practical applications for LTCC is the near-zero temperature coefficient of the resonant frequency (τ_f).[29] Large positive τ_f of $CaTiO_3$ (+859 ppm °C^{-1}) was used as a modifier and was added into $Li_{0.5}(Zn_{0.95}Co_{0.05})_{1.75}SiO_4$ powders doped with 1.5 wt% LMZBS to further adjust the τ_f value (-27.12 ppm °C^{-1}) to around 0 ppm °C^{-1}. The five weight percentages of $CaTiO_3$ were calculated by using the logarithmic rule, where the τ_f value of $Li_{0.5}(Zn_{0.95}Co_{0.05})_{1.75}SiO_4$ was set at -15, -21, -27, -33 and -39 ppm °C^{-1}.

Fig. 8 presents the X-ray diffraction patterns of $(1 - x)$ $Li_{0.5}(Zn_{0.95}Co_{0.05})_{1.75}SiO_4$-$x$ wt% $CaTiO_3$ ceramics doped with 1.5 wt% LMZBS and sintered at 900 °C for 3 h. All the samples exhibited the mixture of $(Zn,Co)_2SiO_4$ (●, PDF #46-1316), $Li_{1.6}Zn_{1.2}SiO_4$ (◆, PDF #24-0676) and $CaTiO_3$ (▽, PDF #39-0145) phases, which indicated that the $CaTiO_3$ phase co-exists with the $Li_{0.5}(Zn_{0.95}Co_{0.05})_{1.75}SiO_4$ ceramic. Furthermore, no other new phase was produced during sintering.

Fig. 9 shows the theoretical and measured τ_f values of $(1 - x)$ $Li_{0.5}(Zn_{0.95}Co_{0.05})_{1.75}SiO_4$-$x$ wt% $CaTiO_3$ ceramics doped with 1.5 wt% LMZBS and sintered at 900 °C for 3 h. The theoretical τ_f values of $(1 - x)Li_{0.5}(Zn_{0.95}Co_{0.05})_{1.75}SiO_4$-$x$ wt% $CaTiO_3$ composite ceramics were calculated using the function (3). As seen in Fig. 9, the theoretical τ_f value of the sample increased with the increasing $CaTiO_3$ content, which resulted from the high τ_f value of $CaTiO_3$.[23] The change in the measured τ_f values showed a similar tendency with the theoretical values, which indicated that the addition of $CaTiO_3$ shifts the τ_f values of $Li_{0.5}(Zn_{0.95}Co_{0.05})_{1.75}SiO_4$ ceramics to positive values. When the

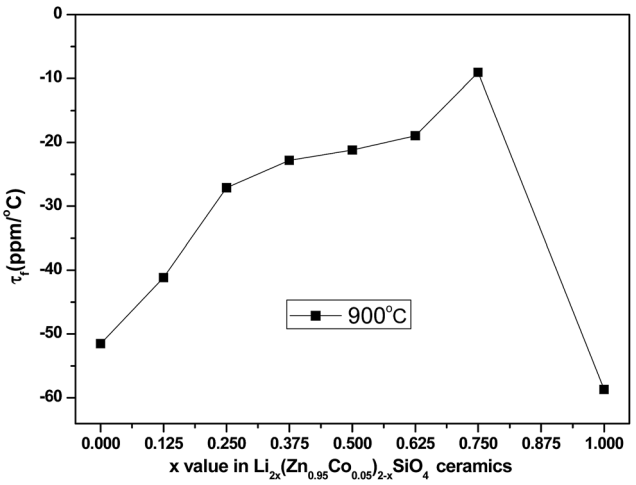

Fig. 7 τ_f values of $Li_{2x}(Zn_{0.95}Co_{0.05})_{2-x}SiO_4$ ($0 \leq x \leq 1$) ceramics doped with 1.5 wt% LMZBS glass and sintered at 900 °C for 3 h.

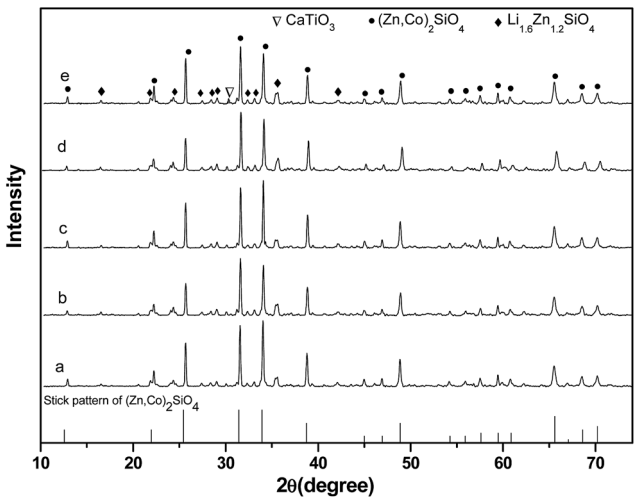

Fig. 8 XRD diffraction patterns of $(1 - x)Li_{0.5}(Zn_{0.95}Co_{0.05})_{1.75}SiO_4$-$x$ wt% $CaTiO_3$ ceramics doped with 1.5 wt% LMZBS and sintered at 900 °C for 3 h. (a) $x = 1.79$, (b) $x = 2.49$, (c) $x = 3.18$, (d) $x = 3.86$ and (e) $x = 4.53$.

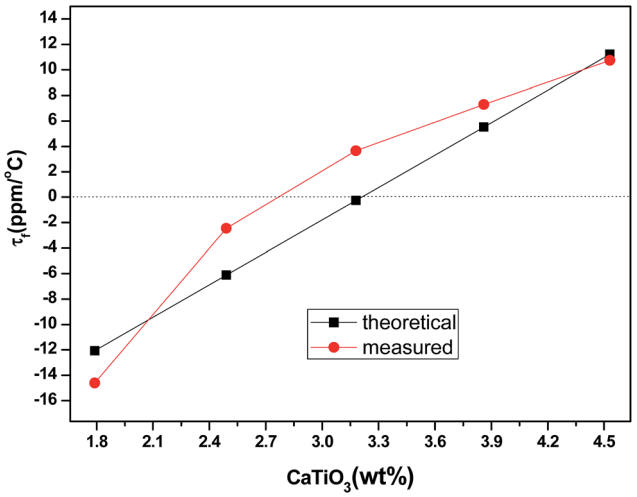

Fig. 9 Theoretical and measured τ_f values of $(1-x)Li_{0.5}(Zn_{0.95}Co_{0.05})_{1.75}SiO_4$-$x$ wt% $CaTiO_3$ ceramics doped with 1.5 wt% LMZBS and sintered at 900 °C for 3 h.

weight percentage of $CaTiO_3$ increased from 1.79 wt% to 4.53 wt%, the measured τ_f values increased from −14.6 ppm °C^{-1} to 10.74 ppm °C^{-1}. A near-zero τ_f value (−2.45 ppm °C^{-1}) was obtained when $x = 2.49$ wt% and the ceramic was sintered at 900 °C for 3 h.

Table 1 shows the theoretical and measured microwave dielectric properties of $(1-x)Li_{0.5}(Zn_{0.95}Co_{0.05})_{1.75}SiO_4$-$x$ wt% $CaTiO_3$ ceramics doped with 1.5 wt% LMZBS and sintered at 900 °C for 3 h. The theoretical permittivities of the composite ceramics were calculated using the function below:[30]

$$\log \varepsilon = v_1 \log \varepsilon_1 + v_2 \log \varepsilon_2 \quad (4)$$

where v_1 and v_2 are the volume fractions and ε_1 and ε_2 are the relative permittivities of the $Li_{0.5}(Zn_{0.95}Co_{0.05})_{1.75}SiO_4$ and $CaTiO_3$ ceramics, respectively. Table 1 shows that the variation of the measured ε_r of $(1-x)Li_{0.5}(Zn_{0.95}Co_{0.05})_{1.75}SiO_4$-$x$ wt% $CaTiO_3$ composite ceramics agrees well with the theoretical value. Given the relatively high ε_r of $CaTiO_3$(162), the measured value increased from 6.47 to 7.152 when the x value increased from 0 wt% to 4.53 wt%. Analogously, the $Q \times f$ values of $(1-x)$ $Li_{0.5}(Zn_{0.95}Co_{0.05})_{1.75}SiO_4$-$x$ wt% $CaTiO_3$ composite ceramics decreased from 131 579 GHz to 41 344 GHz with the increasing x content. This finding is attributed to the low $Q \times f$ value of $CaTiO_3$ (12 000 GHz).[23] Although $CaTiO_3$ adjusted the τ_f values of the $Li_{0.5}(Zn_{0.95}Co_{0.05})_{1.75}SiO_4$ ceramics to nearly zero, the $Q \times f$ values sharply decreased when $CaTiO_3$ was added.

Table 1 Theoretical and measured microwave dielectric properties of the $(1-x)Li_{0.5}$ $(Zn_{0.95}Co_{0.05})_{1.75}SiO_4$-$x$ wt% $CaTiO_3$ ceramics doped with 1.5 wt% LMZBS and sintered at 900 °C for 3 h

Compounds	ε_r (theoretical)	ε_r (measured)	$Q \times f$ values (GHz)
$x = 0$		6.47	131 579
$x = 1.79$	6.838	6.578	74 584
$x = 2.49$	6.987	6.773	69 177
$x = 3.18$	7.137	6.936	57 296
$x = 3.86$	7.289	7.015	51 782
$x = 4.53$	7.441	7.152	41 344

4. Conclusion

The phase evolution and microwave dielectric properties of ceramics with nominal composition $Li_{2x}(Zn_{0.95}Co_{0.05})_{2-x}SiO_4$ were investigated. Lithium ions were added to partly substitute for the zinc ions, and a fixed amount of 1.5 wt% LMZBS glass was used as a sintering aid to help lower the sintering temperature of $Li_{2x}(Zn_{0.95}Co_{0.05})_{2-x}SiO_4$ $(0 \le x \le 1)$ ceramics of around 900 °C. The XRD patterns indicated that various amounts of lithium-ion substitution induce different production patterns of other phases in the $Li_{2x}(Zn_{0.95}Co_{0.05})_{2-x}SiO_4$($0 \le x \le 1$) ceramics. A compact and uniform microstructure with few pores, high relative density and $Q \times f$ value was obtained when x was set at 0.25. The sample exhibited excellent microwave dielectric properties of $\varepsilon_r = 6.47$, $Q \times f = 131\,579$ GHz and $\tau_f = -27.12$ ppm °C^{-1}. In considering the practical application for LTCC, a positive τ_f of $CaTiO_3$ was used to adjust the τ_f value of the composite ceramics to nearly zero. The 1.5 wt% LMZBS-doped 0.975 $Li_{0.5}(Zn_{0.95}Co_{0.05})_{1.75}SiO_4$–0.025$CaTiO_3$ (weight ratio) composite ceramics also presented good dielectric properties of $\varepsilon_r = 6.773$, $Q \times f = 69\,177$ GHz and $\tau_f = -2.45$ ppm °C^{-1}.

Acknowledgements

This work was supported by the National Natural Science Foundation of China under Grant No. 51372031, 61271038 and 51472042, National High-tech R&D Program of China under Grant No. 2015AA034102, Special Support Program of Guangdong Province under Grant No. 2014TX01C042 and Science and Technology Department of Sichuan Province 2014GZ0015, 2015GZ0227.

References

1 W. Lei, W.-Z. Lu, D. Liu and J.-H. Zhu, *J. Am. Ceram. Soc.*, 2009, **92**, 105–109.
2 Y. Zhao and P. Zhang, *RSC Adv.*, 2015, **5**, 97746–97754.
3 T. Tsunooka, M. Androu, Y. Higashida, H. Sugiura and H. Ohsato, *J. Eur. Ceram. Soc.*, 2003, **23**, 2573–2578.
4 O. Yoshihiro, M. Yasuharu, O. Hitoshi and K. Ken-ichi, *Jpn. J. Appl. Phys.*, 2004, **43**, L749.
5 J. C. Kim, M.-H. Kim, S. Nahm, J.-H. Paik, J.-H. Kim and H.-J. Lee, *J. Eur. Ceram. Soc.*, 2007, **27**, 2865–2870.
6 H. Li, W. Lu and W. Lei, *Mater. Lett.*, 2012, **71**, 148–150.
7 J. Guo, D. Zhou, H. Wang and X. Yao, *J. Alloys Compd.*, 2011, **509**, 5863–5865.
8 V. M. Ferreira, F. Azough, J. L. Baptista and R. Freer, *Ferroelectrics*, 1992, **133**, 127–132.
9 Z. Zhang, H. Su, X. L. Tang, H. W. Zhang, T. C. Zhou and Y. L. Jing, *Ceram. Int.*, 2014, **40**, 1613–1617.

10 Y. Guo, H. Ohsato and K.-i. Kakimoto, *J. Eur. Ceram. Soc.*, 2006, **26**, 1827–1830.
11 H. W. Chen, H. Su, H. W. Zhang, T. C. Zhou, B. W. Zhang, J. F. Zhang and X. L. Tang, *Ceram. Int.*, 2014, **40**, 14655–14659.
12 Z. H. Zhou, H. Su, X. L. Tang, H. W. Zhang, F. Xu, S. Zhang and Y. L. Jing, *Ceram. Int.*, 2016, **42**, 11161–11164.
13 J.-j. Bian, D.-W. Kim and K. S. Hong, *Mater. Res. Bull.*, 2005, **40**, 2120–2129.
14 S. George, M. T. Sebastian, S. Raman and P. Mohanan, *Int. J. Appl. Ceram. Technol.*, 2011, **8**, 172–179.
15 S.-H. Kweon, M.-R. Joung, J.-S. Kim, B.-Y. Kim, S. Nahm, J.-H. Paik, Y.-S. Kim and T.-H. Sung, *J. Am. Ceram. Soc.*, 2011, **94**, 1995–1998.
16 S. George, P. S. Anjana, V. N. Deepu, P. Mohanan and M. T. Sebastian, *J. Am. Ceram. Soc.*, 2009, **92**, 1244–1249.
17 E. D. Kim, C. H. Kim and M. H. Oh, *J. Appl. Phys.*, 1985, **58**, 3231–3235.
18 X. C. Fan, X. M. Chen and X. Q. Liu, *IEEE Trans. Microwave Theory Tech.*, 2005, **53**, 3130–3134.
19 Z. Q. Yuan, B. Liu, X. Q. Liu and X. M. Chen, *RSC Adv.*, 2016, **6**, 96229–96236.
20 G. Dou, D. Zhou, S. Gong and M. Guo, *J. Mater. Sci.: Mater. Electron.*, 2012, **24**, 1601–1607.
21 Q. Zeng, W. Li, J.-l. Shi, J.-k. Guo, M.-w. Zuo and W.-j. Wu, *J. Am. Ceram. Soc.*, 2006, **89**, 1733–1735.
22 P. S. Anjana and M. T. Sebastian, *J. Am. Ceram. Soc.*, 2009, **92**, 96–104.
23 C.-H. Hsu, P.-S. Tsai, C.-F. Tseng, S.-H. Hung and I. C. Huang, *J. Alloys Compd.*, 2014, **582**, 355–359.
24 H. L. Pan, Q. Q. Liu, Y. H. Zhang and H. T. Wu, *RSC Adv.*, 2016, **6**, 86889–86903.
25 X. Lu, Y. Zheng, B. Zhou, Z. Dong and P. Cheng, *Ceram. Int.*, 2013, **39**, 9829–9833.
26 H.-H. Xi, D. Zhou, B. He, H.-D. Xie and N. Alford, *J. Am. Ceram. Soc.*, 2014, **97**, 1375–1378.
27 C. Tian, Z. Yue and Y. Zhou, *Mater. Sci. Eng., B*, 2013, **178**, 178–182.
28 B. W. Hakki and P. D. Coleman, *IRE Trans. Microwave Theory Tech.*, 1960, **8**, 402–410.
29 M. Guo, G. Dou, S. Gong and D. Zhou, *J. Eur. Ceram. Soc.*, 2012, **32**, 883–890.
30 Y. Wu, X. Zhao, F. Li and Z. Fan, *J. Electroceram.*, 2003, **11**, 227–239.